NUMERICAL SOLUTION OF A ONE-DIMENSIONAL STEFAN PROBLEM ARISING FROM LASER-ANNEALING

M. BAKKER

1. INTRODUCTION

The problem described here was presented to the author by Frans Saris from Amolf and Wang Zhong Lie (Peking University, from September 1980 to September 1982 working at Amolf). It arose from the research of Laser-annealing of *Si* or *GaAs* whose crystalline structure had been destroyed near the surface by ion-implantation [4,5]. It appears that the crystalline structure recovers after the amorphous layer is irradiated by a laser-beam and is heated to the point of melting. We consider a small piece of *Si* which consists of a thin amorphous layer ($1.5_{10}-5$ cm) at the surface and a relatively thick crystalline layer ($1.185_{10}-3$ cm). When the surface is irradiated by a laser beam of (Gaussian) intensity

$$I(t) = I_0 e^{-(\frac{2\pi I_0(t-t_0)}{E_0})^2} \tag{1.1}$$

with

I_0 maximum intensity in Watt/cm^2
t_0 time at which intensity reaches its peak
E_0 laser energy in Joule/cm^2

the temperature of the *Si* rises and after some time (relatively spoken, the process described takes place within tens of nanoseconds), melting sets in. The melt front (see fig. 1) moves from left to right, until the heating effect due to the laser pulse $I(t)$ dies down and resolidification starts. Then the melt front (it should now be called resolidification front, but for convenience, we will always speak about melt front) moves from right to left until *Si* is solid again.

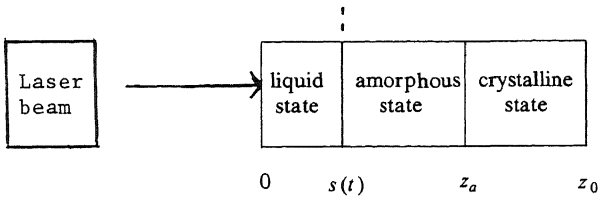

Figure 1.

1.1. Mathematical description of the process

In mathematical terms, the variation of the temperature is described by the heat equation

$$c(T)\rho\frac{\partial T}{\partial t} = \frac{\partial}{\partial z}(\kappa(T)\frac{\partial T}{\partial z}) + S_L(z,t);\ 0<z<z_0;\ t\geqslant 0;$$

$$S_L(z,t) = \alpha(z)e^{-\alpha(z)z}I(t)(1-R); \tag{1.2a}$$

where the parameters have the following meaning:

T	temperature in K;
t	time in seconds;
z	distance from irradiation surface in cm;
z_0	thickness of irradiated *Si*;
$c(T)$	heat capacity of *Si* in Joule/(gram Kelvin); c(T) $>$ 0;
ρ	mass density of *Si* in gram/cm^3 ;
$\kappa(T)$	heat conductivity of *Si* in Watt/(cm Kelvin); $\kappa(T) > 0$;
$\alpha(z)$	absorption coefficient of *Si* in cm $^{-1}$; $\alpha(z) > 0$;
$I(t)$	intensity of laser pulse, defined by (1.1) ;
R	reflectivity of surface; depends on state of surface;
	$R = R_1$,if no melting occurs;
	$R = R_2$,if melting occurs;
	$R_1 > R_2$;

The boundary and initial conditions of T are

$$\begin{aligned} &\frac{\partial T}{\partial z}(0,t) = 0; \\ &T(z_0,t) = T_0\ (= 300K); \\ &T(z,0) = T_0; \end{aligned} \tag{1.2b}$$

where T_0 is the environment temperature.

The two-phase state

If *Si* is only in solid state, equation (1.2a) is valid on $(0,z_0)$ and $\kappa(T)$ and $\partial T / \partial z$ are continuous on $(0,z_0)$, while the forcing term $S_L(z,t)$ may be discontinuous at some points, e.g. at the amorphous-crystalline interface. If melting occurs, however, these expressions are discontinuous at the melt front $s(t)$, where the Stefan interface conditions hold:

$$T(s(t),t) = T_m\ (= 1685K); \tag{1.2c}$$

$$L_0\rho\dot{s}(t) = \lim_{z\downarrow s(t)}[\kappa(T)\frac{\partial T}{\partial z}] - \lim_{z\uparrow s(t)}[\kappa(T)\frac{\partial T}{\partial z}] \tag{1.2d}$$

with

L_0	latent heat of *Si* in J/g;
$\dot{s}(t)$	$ds(t)/dt$, the speed of the melt front;
T_m	melt temperature of *Si*;

Discontinuities of κ(T) and α(z) at melt front

In the current model, the absorption coefficient α is supposed to be a piecewise constant function defined by

$$\alpha(z) = \begin{cases} \alpha_s \ (=5.0_{10}4) & , \text{if } s(t) < z \leqslant z_0; \\ \alpha_m \ (=7.0_{10}5) & , \text{if } 0 \leqslant z < s(t) \end{cases} \tag{1.3}$$

The heat conductivity is defined by

$$\kappa(T) = \begin{cases} \kappa_m (=0.51) & , \text{if } T > T_m; \\ \kappa_s(T) & , \text{if } T_0 \leqslant T < T_m; \end{cases} \tag{1.4}$$

where κ_s is positive , continuous and monotonically decreasing on $[T_0,T_m]$ with

$$\lim_{T \uparrow T_m} \kappa_s(T) \neq \kappa_m.$$

1.2. Limitations of the model

The above model of the heat conduction by laser-iradiated *Si* is a deliberate simplification, since only the mathematical aspects are now being discussed. The simplifications are:

1. Evaporation of *Si* is not taken into account, while as a matter of fact, it evaporates if E_0 is large enough.
2. α_s is assumed to be constant on $(s(t),z_0)$, while in reality α_s has a discontinuity at the crystalline-amorphous interface.
3. The melt temperature of *Si* is assumed to be the same for amorphous and crystalline *Si*, while the amorphous melt temperature is some hundreds of degrees lower than the crystalline melt temperature (1373 K vs. 1685 ° K).
4. $\kappa_s(T)$ is discontinuous at the amorphous-crystalline interface, while in this paper it is supposed to be continuous on $[s(t),z_0]$.

2. NUMERICAL SOLUTION OF THE MOVING BOUNDARY PROBLEM

There are some pitfalls for the numerical analyst, when he tries to solve this problem per computer:

1. The appearance and disappearance of the melt front.

   Before and after the melting, the Boundary Problem is standard. It is, however, impossible to establish beforehand when the melting commences and terminates. Consequently, after each timestep, the state of the system has to be checked:

   a. Is the temperature at the surface (where it is hottest) still below T_m ? (only relevant, if the temperature is rising and if there is no liquid state).

   b. Is the melt front still present?

2. The presence of a moving material interface inside $(0,z_0)$ makes it impossible to use standard semi-discretization and time-integration methods.

   The use of a variable space-grid which was successfully practiced by Bonerot & Jamet [2], fails here because of the initial and final tininess of the liquid region $(0,s(t))$.

2.1. Transformation of the space variable

A well known method for coping with MBPs is the use of transformations replacing variable domains by fixed domains. In this case, we introduce the transformations

$$z = \begin{cases} xs(t) & , \text{if } z \leqslant s(t); \\ xz_0 + (1-x)s(t) & , \text{if } z \geqslant s(t). \end{cases} \tag{2.1}$$

Furthermore, we split T in T_s and T_l by

$$T = \begin{cases} T_l & , \text{if } z \leqslant s(t); \\ T_s & , \text{if } z \geqslant s(t). \end{cases} \tag{2.2}$$

After some calculus, problem (1.2) is transformed to the following system of problems:

$$\begin{aligned} & c(T_l)\rho[\frac{\partial T_l}{\partial t} - \frac{x\dot{s}}{s}\frac{\partial T_l}{\partial x}] = \frac{\kappa_m}{s^2}\frac{\partial^2 T_l}{\partial x^2} + \\ & \quad + \alpha_m(1-R)I(t)e^{-\alpha_m xs}; \\ & \frac{\partial T_l}{\partial x}(0,t) = 0;\ T_l(1,t) = T_m; \end{aligned} \tag{2.3}$$

$$\begin{aligned} & c(T_s)\rho[\frac{\partial T_s}{\partial t} - \frac{(1-x)\dot{s}}{z_0-s}\frac{\partial T_s}{\partial x}] = \frac{1}{(z_0-s)^2}\frac{\partial}{\partial x}(\kappa_s(T_s)\frac{\partial T_s}{\partial x}) + \\ & \quad + \alpha_s(1-R)I(t)e^{-\alpha_s(xz_0+(1-x)s)}; \\ & T_s(0,t) = T_m;\ T_s(1,t) = T_0; \end{aligned} \tag{2.4}$$

$$L_0\rho\dot{s} = \frac{\kappa_s(T_m)}{z_0-s}\frac{\partial T_s}{\partial x}(0,t) - \frac{\kappa_m}{s}\frac{\partial T_l}{\partial x}(1,t). \tag{2.5}$$

We see that by the use of (2.1), we have transformed (1.2) into a system of two transient boundary problems and one *Ordinary Differential Equation* (ODE).

2.2. The discrete time Galerkin method

If s(t) were always positive, problems (2.3)-(2.5) could be semi-discretized in space by some standard method and afterwards integrated in time by some ODE integrator. However, s(t) starts and ends with a zero value which makes (2.3) singular. We therefore introduce a *discrete time method:* we approximate $\partial T_l / \partial t$ and $\partial T_s / \partial t$ by some difference method and hence solve the resulting system of ODEs.

For the time-discretization, we choose the *Backward Euler Method:*

$$\frac{\partial T_l}{\partial t}(x,t) \approx \frac{T_l(x,t) - T_l(x,t-\tau)}{\tau};\ \frac{\partial T_s}{\partial t}(x,t) \approx \frac{T_s(x,t) - T_s(x,t-\tau)}{\tau}; \tag{2.6}$$

Substitution of (2.6) in (2.3) and (2.4) leads to a system of *Two Point Boundary Problems*

$$c(T_l)\rho[\frac{T_l-T_l^*}{\tau} - \frac{x\dot{s}}{s}T_l'] =$$

$$= \frac{\kappa_m}{s^2}T_l'' + \alpha_{in}(1-R)I(t)e^{-\alpha_m xs}; \tag{2.7}$$

$$T_l'(0) = 0;\ T_l(1) = T_m;$$

$$c(T_s)\rho[\frac{T_s-T_s^*}{\tau} - \frac{(1-x)\dot{s}}{z_0-s}T_s'] =$$

$$= \frac{1}{(z_0-s)^2}(\kappa_s(T_s)T_s')' + \alpha_s(1-R)I(t)e^{-\alpha_s[xz_0+(1-x)s]}; \tag{2.8}$$

$$T_s(0) = T_m;\ T_s(1) = T_0;$$

$$L_0\rho\dot{s} = \frac{\kappa_s(T_m)}{z_0-s}T_s'(0) - \frac{\kappa_m}{s}T_l'(1). \tag{2.9}$$

In (2.7) and (2.8), T_l, T_s, T_l^* and T_s^*, denote $T_l(x,t)$, $T_s(x,t)$, $T_l(x,t-\tau)$ and $T_s(x,t-\tau)$, respectively.

The problems (2.7)-(2.8) can be solved by some space discretization method. This method can be the Finite Difference Method (FDM) or the Finite Element Method (FEM) [6] . We prefer the latter method, not solely for reasons of taste but because it enables us to approximate $\dot{s}$ more accurately, as we will show.

2.2.1. The Finite Element Method using piecewise linear functions

Let

$$\Delta = \{0=x_0 < x_1 < \cdots < x_N = 1\} \tag{2.10}$$

be a uniform partition of [0,1] in N segments with

$$x_i = hi;\ i = 0,\cdots,N;\ h = 1/N; \tag{2.11}$$

If we put

$$T_l(x_i,t) \approx U_i;\ T_l(x_i,t-\tau) \approx U_i^*;$$

$$T_s(x_i,t) \approx V_i;\ T_s(x_i,t-\tau) \approx V_i^*;\ i = 0,\ \cdots,\ N. \tag{2.12}$$

Then, for $\vec{U}$ and $\vec{V}$, the following difference scheme results from application of the C^0 Galerkin method using piecewise linear functions on Δ:

$$c(U_0)\rho\frac{h}{2}[(U_0-U_0^*)/\tau] = \frac{\kappa_m}{s^2}\frac{U_1-U_0}{h} + \frac{h}{2}\alpha_m I(t)(1-R);$$

$$c(U_i)h\,\rho[(U_i-U_i^*)/\tau - \frac{x_i\dot{s}}{s}\frac{U_{i+1}-U_{i-1}}{2h}] =$$

$$= \frac{\kappa_m}{s^2}\frac{U_{i+1}-2U_i+U_{i-1}}{h} + h\alpha_m I(t)(1-R)e^{-\alpha_m s x_i};\ 1 \leqslant i \leqslant N-1; \tag{2.13}$$

$$U_N = T_m;$$

$$c(V_i)\rho h\left[\frac{V_i - V_i^*}{\tau} - \frac{(1-x_i)\dot{s}}{z_0 - s}\frac{V_{i+1}-V_{i-1}}{2h}\right] =$$

$$= \frac{(\kappa_s(V_{i-1})+\kappa_s(V_i))(V_{i-1}-V_i) + (\kappa_s(V_{i+1})+\kappa_s(V_i))(V_{i+1}-V_i)}{2(z_0-s)^2 h} + \tag{2.14a}$$

$$+ h(1-R)\alpha_s I(t)e^{-\alpha_s[x_i z_0 + (1-x_i)s]};\ 1 \leqslant i \leqslant N-1;$$

$$V_0 = T_m;\ V_N = T_0.$$

If no melting occurs and if we apply the same discrete time Galerkin method, we obtain for $\vec{V}$ the linear system

$$c(V_0)\rho h\frac{V_0 - V_0^*}{2\tau} = \frac{(\kappa_s(V_0)+\kappa_s(V_1))(V_1-V_0)}{2z_0^2 h} +$$

$$+ \tfrac{1}{2}h(1-R)\alpha_s I(t);$$

$$c(V_i)\rho h\left[\frac{V_i - V_i^*}{\tau}\right. =$$

$$= \frac{[\kappa_s(V_{i-1})+\kappa_s(V_i)](V_{i-1}-V_i) + [\kappa_s(V_{i+1})+\kappa_s(V_i)](V_{i+1}-V_i)}{2z_0^2 h} + \tag{2.14b}$$

$$+ h(1-R)\alpha_s I(t)e^{-\alpha_s x_i z_0};\ 1 \leqslant i \leqslant N-1;$$

$$V_N = T_0.$$

Note that in (2.14b) V_0 is now variable, because of the natural boundary condition (1.2b) for $z = 0$.

2.2.2. Approximation of ṡ

In (2.13)-(2.14) $\dot{s}$ has yet to be approximated by some difference expression. It would be ıpting to use some finite difference formula for $\dot{s}$ like

$$L_0\rho\dot{s} \approx \frac{\kappa_s(V_0)(V_1-V_0) - \kappa_m(U_N - U_{N-1})}{h}. \tag{2.15}$$

This formula, however, has the disadvantage that the approximation of $\dot{s}$ is one order less accurate than the approximation of T_s and T_l, i.e. of $O(h)$ vs. $O(h^2)$.

In order to obtain a better approximation of $\dot{s}$, we use a result of Wheeler [3] which consists of a cheap and accurate approximation of the flux at the break-points x_i, once the Galerkin solution is known (see the Appendix for a more extensive treatment). If we apply their theorem to (2.13) and (2.14), we obtain the following approximations for $T_l'(1,t)$ and $T_s'(0,t)$:

$$\frac{\kappa_m}{s}T_l'(1) \approx \frac{\kappa_m(U_N - U_{N-1})}{hs} +$$

$$+ \tfrac{1}{2}[\alpha_m hsI(t)(1-R)e^{-\alpha_m s} - \dot{s}c(U_N)\rho(U_N - U_{N-1})]; \tag{2.16}$$

$$\frac{\kappa_s(T_m)}{z_0-s}T_s'(0,t) \approx \frac{[\kappa_s(V_0)+\kappa_s(V_1)](V_1-V_0)}{2h(z_0-s)} +$$

$$+ \tfrac{1}{2}[\dot{s}c(V_0)\rho(V_0-V_1) + h(z_0-s)\alpha_s I(t)(1-R)e^{-\alpha_s s}]; \tag{2.17}$$

If we subtract (2.16) from (2.17), we easily find that

$$\dot{s}[L_0\rho + \tfrac{1}{2}c(T_m)(U_{N-1}-V_1)] \approx$$

$$\approx \frac{[\kappa_s(V_0)+\kappa_s(V_1)](V_1-V_0)}{2h(z_0-s)} - \frac{\kappa_m(U_N-U_{N-1})}{hs} + \tag{2.18}$$

$$+ \tfrac{1}{2}hI(t)(1-R)[\alpha_m s e^{-\alpha_m s} + \alpha_s(z_0-s)e^{-\alpha_s s}]$$

which yields an approximation of $\dot{s}$ which is not only more accurate than (2.15) but works better at the early stage of the melting state.

2.3. Iteration scheme for time-integration

As we saw in the previous section, time-integration is easy enough, if $s(t)=0$. If melting occurs, we use for the solution of (2.13)-(2.14) and (2.18) the following scheme (see also Bonerot & Jamet [2]) :

<table>
<tr><td colspan="2">Make an initial guess of s by
$s_0(t)=s(t-\tau)+\tau\dot{s}_0(t)$; $\dot{s}_0(t)=\dot{s}(t-\tau)$
Make an initial guess of $\vec{U}$ and $\vec{V}$ by putting $\vec{U}^0 = \vec{U}^*$ and $\vec{V}_0 = \vec{V}^*$.</td></tr>
<tr><td rowspan="2">Repeat until some stop criterion is satisfied</td><td>Perform one Newton iteration for the solution of (2.13)-(2.14) for $s = s_i(t)$, $\dot{s} = \dot{s}_i(t)$, to obtain $\vec{U}^{i+1}$ and $\vec{V}^{i+1}$, $i = 0, \cdots,$</td></tr>
<tr><td>Compute $\dot{s}_{i+1}(t)$ from (2.18) for $\vec{U}^{i+1}$ and $\vec{V}^{i+1}$ and put $s_{i+1}(t)=s(t-\tau)+\tau\dot{s}_{i+1}(t)$</td></tr>
</table>

Table 1. Iteration scheme for time-integration

We see that the above iteration scheme reduces to a common Newton iteration process, if we delete the updating of $\vec{U}$, $s(t)$ and $\dot{s}(t)$ from it.

There is only one small problem in the iteration scheme of table 1: how to get a reasonable guess of $\dot{s}$ when, the melting starts? One could try to extrapolate formula (2.18) to $s=0$. Another method is the following: One can easily derive from (1.2) the ODE

$$\begin{aligned}&\frac{d}{dt}[L_0\rho s(t) + \int_0^{z_0} T(z,t)dz] = \\ &= \int_0^{z_0} S_L(z,t)dz + \kappa_s(T_0)\frac{\partial T}{\partial z}(z_0,t) = \\ &= (1-R)I(t)(1-e^{-\alpha_m s}+e^{-\alpha_s s}-e^{-\alpha_s z_0}) + \kappa_s(T_0)\frac{\partial T}{\partial z}(z_0,t).\end{aligned} \tag{2.19}$$

If we cancel $\frac{\partial T}{\partial z}(z_0,t)$ in (2.19) and cancel the variation of $\int_0^{z_0} T(z,t)dz$, we have the approximation

$$L_0\rho\dot{s}(t) \approx (1-R)I(t)(1-e^{-\alpha_s z_0}), \text{ if } s(t) = 0. \tag{2.20}$$

REMARK

Formula (2.20) is an overestimation of $\dot{s}$ but has the advantage that its order of magnitude is not wildly misguessed.

2.4. Stepsize control

In order to control the time-integration process, the following conditions were imposed to the stepsize τ :

1. The surface temperature T(0,t) is not allowed to change by more than, say, 100 K. If so, the time-step is rejected and, by interpolation, a new and smaller time-step is tried.
2. The melt front is not allowed to change by more than , say, 50 Angstroem. If so, the time-step is rejected and, by interpolation, a new and smaller time-step is tried.
3. τ has the bounds

$$1.0_{10}-12 = \tau_{\min} \leqslant \tau \leqslant \tau_{\max} = 10.0(hz_0)^2$$

4. τ is not allowed to increase by more than 50 % per timestep.
5. If the state of the system changes between $t-\tau$ and t, t is rejected and , by interpolation, replaced by a new t which is a prediction of the time at which the change takes place. For example, if

   $V_0^* < T_m < V_0$;

   where $\vec{V}$ is the solution of (2.14b), then τ is replaced by

$$\tau^* = \frac{(T_m - V_0^*)\tau}{V_0 - V_0^*}.$$

3. NUMERICAL EXAMPLE

In this chapter, problem (1.2) is numerically solved for the following input parameters:

Parameter	value or domain
T_0	300 K
T_m	1685 K
t_0	25 νs
I_0	$5.0_{10}7$
z_0	$1.2_{10}-3$ cm
ρ	2.33
E_0	0.5,1,1.5,2,2.5 Joule
κ_m	0.51
α_m	$7.0_{10}5$
α_s	$5.0_{10}4$
L_0	1801
κ_s	$1.38 \geqslant \kappa_s \geqslant 0.32$
	κ_s monotonically decreasing on (T_0,T_m)
c(T)	$0.95 \leqslant c(T) \leqslant 1.10$
	c monotonically increasing on $[T_0,\infty)$
R	R = 0.3, if no melting occurs;
	R = 0.6, if *Si* is melting

From the graphs of $s(t;E_0)$ (see fig. 2) and $T(0,t;E_0)$ (see fig. 3) one can see that

1. The melting starts sooner, the melt depth is larger and the melting ends later, when E_0 is larger;
2. The surface temperature has a larger peak, if E_0 is larger.

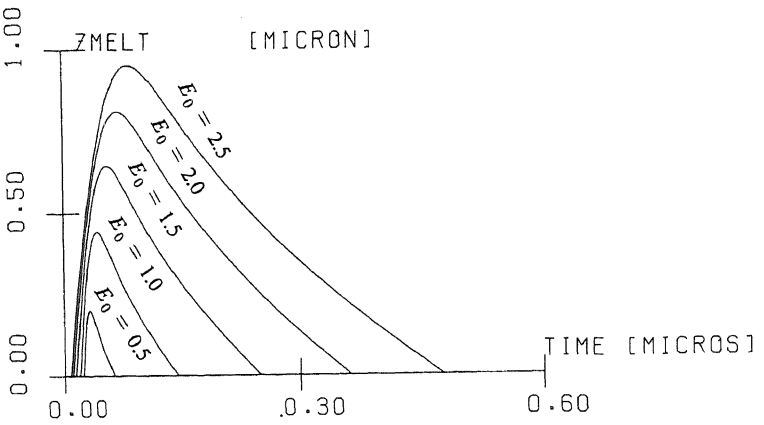

Figure 2. Graph of $s(t)$ for $E_0 = 0.5,1.0,1.5,2.0,2.5$

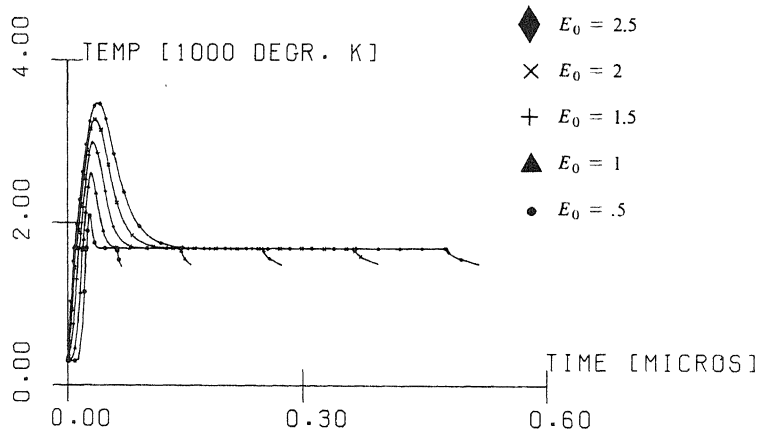

Figure 3. Graph of $T(0,t)$ for $E_0 = 0.5,1.0,1.5,1.0,1.5$

REFERENCES

[1] ABRAMOWITZ, M. & I. STEGUN, *Handbook of Mathematical Functions,* Dover Publications, 1964.

[2] BONEROT, R. & P. JAMET, *A Second Order Finite Element Method for the One-Dimensional Stefan Problem,* Internat. J. Numer. Methods Engrg. **17** (1981), 811-820;

[3] CAREY, G.F., D. HUMPHREY & M.F. WHEELER, *Galerkin and Collocation-Galerkin Methods with Superconvergence and Optimal Fluxes,* Internat. J. Numer. Methods Engrg. **8** (1974), 939-950;

[4] GILES, G.E.& R.F. WOOD, *Macroscopic Theory of Pulsed Laser Annealing,* Phys. Rev B **3** (1981), 2923-2942;

[5] DE JONG, T., WANG Z.L. & F.W. SARIS, *An experimental test of GaAs decompostion due to pulsed laser irradiation,* to appear in Physical Letters

[6] MITCHELL, A.R. & R. WAIT, *The Finite Element Method in Partial Differential Equations,* John Wiley & Sons, Chichester, New York, Brisbane, Toronto, 1977;

APPENDIX

Let

$$-(p(x)y')' + q(x)y' + r(x)y = f(x),\ x \in (0,1); \tag{A1}$$

$$y(0) = y(1) = 0; \tag{A2}$$

be some two-point boundary problem with unique solution. Then for every $\phi \in C^0(0,1)$ the relation

$$(py',\phi') + (qy',\phi) + (ry,\phi) = (f,\phi) + [p(x)y'(x)\phi(x)]_0^1 \tag{A3}$$

holds, where (.,.) denotes the usual $L^2(I)$ inner product.

Let Δ defined by (2.10)-(2.11) , be a partition of [0,1] and let ϕ_i, $i = 0, \cdots, N$ be defined by

$$\phi_0(x) = \begin{cases} 1-x/h & , \text{if } 0 \leqslant x \leqslant h; \\ 0 & , \textit{elsewhere}; \end{cases} \tag{A4}$$

$$\phi_i(x) = \begin{cases} (x-x_{i-1})/h & , \text{if } x_{i-1} \leqslant x \leqslant x_i; \\ (x_{i+1}-x)/h & , \text{if } x_i \leqslant x \leqslant x_{i+1}; \\ 0 & , \textit{elsewhere}; i = 1, \cdots, N-1; \end{cases} \tag{A5}$$

$$\phi_N(x) = \begin{cases} (x-_{N-1})/h & , \text{if } x_{N-1} \leqslant x \leqslant 1; \\ 0 & , \textit{elsewhere}; \end{cases} \tag{A6}$$

Then it is standard [6] that y(x) can be approximated by

$$Y(x) = \sum_{i=1}^{N-1} c_i \phi_i(x); \tag{A7}$$

where $\vec{c}$ is the solution of the (tri-diagonal) linear system

$$\sum_{j=1}^{N-1} [(p\phi'_i,\phi'_j) + (q\phi_i,\phi'_j) + (r\phi_i,\phi_j)]c_j = (f,\phi_i),\ i = 1,\cdots,N-1. \tag{A8}$$

The pointwise error of Y is

$$|y(x) - Y(x)| \leqslant C(y)h^2,\ x \in [0,1]; \tag{A9}$$

For the boundary fluxes, Wheeler[3] developed the approximations

$$\begin{aligned} -p(0)y'(0) &\approx (pY',\phi'_0) + (qY',\phi_0) + (rY,\phi_0) - (f,\phi_0); \\ +p(1)y'(1) &\approx (pY',\phi'_N) + (qY',\phi_N) + (rY,\phi_N) - (f,\phi_N); \end{aligned} \tag{A10}$$

by simply applying (A3) for ϕ_0 and ϕ_N and replacing y by Y in the integrand. She could prove that (A10) has an approximation error of $0(h^2)$ instead of $O(h)$ which would have been achieved if the difference formulae

$$\begin{aligned} y'(0) &\approx (c_1 - c_0)/h; \\ y'(1) &\approx (c_N - c_{N-1})/h \end{aligned} \tag{A11}$$

were used.

In (A9-A10), integrals involving p,q,r,f are to be evaluated, which can sometimes be cumbersome. However, if in formulae (A9-A10) (.,.) is approximated by the extended trapezoid rule [1,ch. 25.4.2], the orders of accuracy remain $O(h^2)$.

If the above formulae are applied to (2.7)-(2.9) with use of the extended trapezoidal formula, equations (2.13)-(2.14) and (2.16)-(2.18) result.